Bone Reports 14 (2021) 100738

Contents lists available at ScienceDirect

Bone Reports

journal homepage: www.elsevier.com/locate/bonr

Case Report

Challenges in long-term control of hypercalcaemia with denosumab after haematopoietic stem cell transplantation for *TNFRSF11A* osteoclast-poor autosomal recessive osteopetrosis

Tashunka Taylor-Miller [a], Ponni Sivaprakasam [b], Sarah F. Smithson [c,d], Colin G. Steward [d,e], Christine P. Burren [a,d,*]

[a] Department of Paediatric Endocrinology, Bristol Royal Hospital for Children, University Hospitals Bristol and Weston NHS Foundation Trust, Bristol, United Kingdom
[b] Paediatric Bone Marrow Transplant Service, Bristol Royal Hospital for Children, University Hospitals Bristol and Weston NHS Foundation Trust, Bristol, United Kingdom
[c] Department of Clinical Genetics, St Michaels Hospital, University Hospitals Bristol and Weston NHS Foundation Trust, Bristol, United Kingdom
[d] Bristol Medical School: Translational Health Sciences, University of Bristol, Bristol, United Kingdom
[e] School of Cellular and Molecular Medicine, University of Bristol, Queens Road, Bristol BS8 1QU, United Kingdom

ARTICLE INFO

Keywords:
Craniosynostosis
Denosumab
Haematopoietic stem cell transplantation
Hypercalcaemia
Osteopetrosis
TNFRSF11A

ABSTRACT

Autosomal recessive osteopetrosis (ARO) is rare, involving increased bone density due to defective osteoclast differentiation or function, with several genetic subtypes.

Case: This child with compound heterozygous novel loss-of-function *TNFRSF11A* pathogenic variants causing osteoclast-poor ARO underwent haematopoietic stem cell transplantation (HSCT) aged 3.1 years and experienced episodic severe hypercalcaemia over 2.5 years. She initially presented aged 8 months with craniosynostosis and visual impairment and underwent surgery; no increased bone density evident on skull imaging nor variants in genes associated with craniosynostosis identified. She was subsequently referred for investigation of poor linear growth and low alkaline phosphatase. Clinical abnormalities included asymmetric pectus carinatum, thickened anterior tibia and wrists, and markedly delayed dentition. Skeletal survey revealed generalised osteosclerosis with undertubulation.

Management: She received haploidentical HSCT aged 3.1 years and developed hypercalcaemia (adjusted calcium 4.09mmol/L = 16.4mg/dL) Day 18 post-HSCT, unresponsive to hyperhydration and diuretics. Denosumab achieved normocalcaemia, which required 0.6mg/kg every 6 weeks long-term. The ensuing 2.75 years feature full donor engraftment, good HSCT graft function, skeletal remodelling with 2.5 years recurrent severe hypercalcaemia and nine fragility long bone fractures.

Conclusion: This case illustrates challenges of bone and calcium management in ultrarare *TNFRSF11A*-related OP-ARO. Craniosynostosis was an early feature, evident pre-sclerosis in osteopetrosis. Following HSCT, restoration of osteoclast activity in the context of elevated bone mass produced severe and prolonged (2.5 years) hypercalcaemia. Denosumab was effective medium-term, but required concurrent long duration (11 months) zoledronic acid to manage recurrent hypercalcaemia. Fragility fractures brought appreciable additional morbidity in the post-HSCT phase.

1. Introduction

Autosomal recessive osteopetrosis (ARO) is rare (1:250,000), usually presents in infancy, requiring prompt diagnosis to facilitate early haematopoietic stem cell transplantation (HSCT) where appropriate (Wu et al., 2017). Hypercalcaemia can emerge once HSCT for ARO restores osteoclast activity (Martinez et al., 2010). Whilst hypercalcaemia may occur in various types of ARO, it is especially the case in the osteoclast-poor forms and can be particularly severe in the OP-ARO subtype due to mutations in the Tumour Necrosis Factor Receptor Superfamily 11A (*TNFRSF11A*) gene, which encodes the protein Receptor Activator of NF-kB (RANK) (Shroff et al., 2012; Pangrazio et al., 2012; Paul et al., 2019).

* Corresponding author at: Bristol Royal Hospital for Children, Bristol BS2 8BJ, United Kingdom.
E-mail address: Christine.burren@uhbw.nhs.uk (C.P. Burren).

https://doi.org/10.1016/j.bonr.2020.100738
Received 20 August 2020; Received in revised form 22 November 2020; Accepted 28 November 2020
Available online 2 December 2020

Rapid onset severe hypercalcaemia is a medical emergency: patients can be unwell, thirsty, dehydrated and have abdominal pain; complications include pre-renal renal failure, nephrocalcinosis and long-term renal impairment (Martinez et al., 2010). So, vigilance in calcium monitoring and appropriate management of hypercalcaemia is required.

The monoclonal antibody denosumab mimics osteoprotegerin action by blocking RANK ligand (RANKL) binding to RANK receptor, thus inhibiting osteoclast differentiation, activity, and bone resorption. The mean half-life of denosumab from adult data is 29 days (range 25–35 days). In vivo development of antibodies against denosumab that might influence efficacy has not been described. Functional inhibition of bone turnover rapidly reverses after drug discontinuation, in contrast to bisphosphonates which persist in bone (Boyce, 2017). Other case reports of denosumab use in children with refractory post-HSCT-hypercalcaemia with short to medium term follow-up (Shroff et al., 2012; Pangrazio et al., 2012; Paul et al., 2019) suggest hypercalcaemia may resolve by 9–12 months allowing denosumab discontinuation. We report an extremely unusual and challenging OP-ARO case with longer duration (2.5 years post-HSCT) of problematic hypercalcaemia despite 18 months of denosumab, then 12 months of adjuvant zoledronic acid. This case contributes new information on denosumab dose and frequency in a <10 kg patient. It demonstrates that rebound hypercalcaemia may occur despite concomitant bisphosphonate therapy, and may be prolonged in the setting of markedly elevated bone mass. Osteoclast remodelling of osteopetrotic bone post-HSCT should ultimately lessen excessive bone mass, but our case illustrates the attendant risk of deleterious severe hypercalcaemia and the fragility fractures (due to low-energy trauma) highlight the underlying abnormal bone quality. This *TNFRSF11A* OP-ARO case illustrates the complexity of a bone metabolism medication strategy which optimally controls osteoclasts to resolve hypercalcaemia whilst sufficiently permissive of skeletal remodelling post-HSCT. This case also adds evidence to the literature that craniosynostosis may constitute an early feature of ARO.

2. Case report

A now 5.9-year-old girl was referred to paediatric endocrine services aged 2.3 years due to poor linear growth and concern around low alkaline phosphatase. She had no bone pain and consumed a normal calcium content diet. She was born at 41 weeks gestation with normal birth weight (3.57 kg), of mixed White British and British Asian ethnicity. During her early months she was assessed for a left intermittent divergent squint, with otherwise normal developmental milestones and growth in infancy. She then presented aged 8 months with a bulging fontanelle and cranial imaging identified bilateral partial coronal craniosynostosis without hydrocephalus. Plain radiograph imaging did not give evidence of any skull vault or skull base density increase (Fig. 1A). Ophthalmology assessment revealed nystagmus, left visual impairment and optic nerve pallor. CT imaging (not shown) did not give any evidence of foraminal narrowing; it remained unclear whether the optic

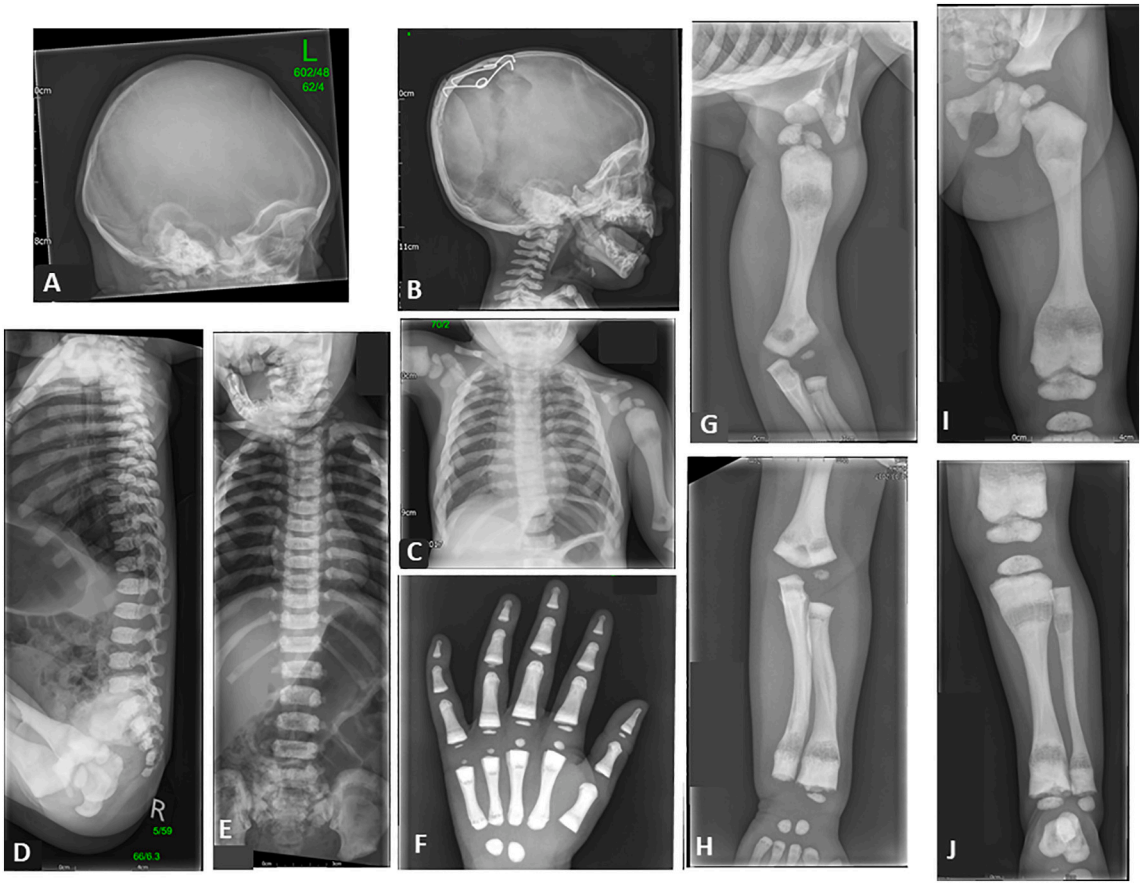

Fig. 1. Radiology: initial lateral skull plain radiograph aged 8 months on presentation with craniosynostosis; no increased density of either skull vault or skull base evident on this radiograph [A]. Remainder are skeletal survey plain radiographs at diagnosis of osteopetrosis aged 2.3 years; all show marked generalised increased density (B–J). B: Increased skull base density with skull vault sparing, previous skull vault surgical springs. C Chest X-ray: increased rib density, proximal humeral medullary lucencies. Spine shows mild platyspondyly and end-plate sclerosis and bone in bone appearance in the pelvis (lateral [D] and PA [E]). Hand and wrist [F]: increased density throughout all carpal, metacarpal and phalanges. Long bone images (humerus [G], radius and ulna [H], femur [I], tibia and fibula [J]) show loss of corticomedullary differentiation and undertubulation with prominent medullary lucencies in proximal and distal diaphyses. (Image [I] of the femur also shown in Fig. 3(last panel) for comparison to illustrate long bone growth between baseline and 2.5 years post-HSCT).

nerve dysfunction was due to raised intracranial pressure or a degree of foraminal narrowing or a combination thereof. Visual loss progressed. Craniofacial surgery was undertaken, involving posterior vault expansion, due to progressive suture involvement (lambdoid and squamous sutures). Clinical examination aged 2.3 years showed significant short stature (height z score −3.4 SDS, weight z score −4.9 SDS, BMI 14.14 kg/m^2 [2nd centile], head circumference 46.6 cm[50th centile]), asymmetric pectus carinatum, mild facial asymmetry, markedly delayed primary dentition (only 3 erupted teeth), mild thickening and broadening of wrists and anterior tibia, but no significant bowing or marked other deformity. She had severe but stable visual impairment, bilateral optic atrophy and retained light perception in left eye.

Investigations: initial testing prior to the craniosynostosis surgery had shown a normal array CGH (Comparative genomic hybridization) and a craniosynostosis gene panel had identified no causative variants, including extended sequencing of *TCF12*, *FGFR2* and *ERF* genes. Biochemistry investigations aged 2 years indicated persistently mildly low alkaline phosphatase (94–139 IU/L, reference range 156–369), normal full blood count, electrolytes and liver function. A skeletal survey aged 2.3 years revealed marked generalised increased density of the appendicular and axial skeleton, bone in bone appearance in the pelvis, long bones showed loss of corticomedullary differentiation and undertubulation with prominent medullary lucencies in proximal and distal diaphyses, and spine showed mild platyspondyly and end-plate sclerosis (Fig. 1 panels B–J). This radiological evidence suggested a form of osteopetrosis or 'sclerosing skeletal dysplasia', highlighting that osteopetrosis and dysosteosclerosis are overlapping entities. This case was diagnostically challenging, as the absence of initial osteosclerosis on imaging under one year of age, and the lack of hepatosplenomegaly and hypogammaglobulinaemia were consistent with dysosteosclerosis, whereas in our opinion the platyspondyly was much more minimal than typical for dysosteosclerosis. Molecular genetic testing was undertaken on a clinical basis by the Bristol Genetics Laboratory with a bespoke panel for osteopetrosis and osteosclerosis using Agilent's Focused Exome custom target enrichment system SureSelectXT for the following 21 genes: *ANKH, CA2, CLCN7, CTSK, FAM123B, FAM20C, FERMT3, IKBKG, LEMD3, LRP5, OSTM1, SNX10, SOST, TCIRG1, TGFB1, PLEKHM1, PTH1R, RASGRP2, TNFRSF11A, TNFSF11, TYROBP,* and variants confirmed using Sanger Sequencing. This revealed two compound heterozygous variants in *TNFRSF11A* gene not reported in other patients: c.414_427 + 7del, p.(Gln140Alafs*17) (maternal, White British ethnicity) and c.1664del, p.(Ser555Cysfs*121) (paternal, British Asian ethnicity). These describe deletions predicted to cause frameshifts resulting in STOP codons 16 and 120 bps downstream respectively, resulting in reduced or absent *TNFRSF11A* expression and were classified as pathogenic and likely pathogenic respectively according to American College of Medical Genetics and Genomics (ACMG) Guidelines (Richards et al., 2015) and Association for Clinical Genomic Science (ACGS): c.414_427 + 7del [p.Gln140Alafs*17] (ACGS 2019 scoring PM2 (moderate pathogenicity) absent gnomAD reference population, PVS1 (Pathogenic Very Strong) nonsense mediated decay predicted due to disruption of donor site exon 4 of 10, not reported in other patients, pathogenic) and c.1664del [p.Ser555Cysfs*121] (ACGS 2019 scoring PM2 absent gnomAD reference population, PVS1_moderate nonsense mediated decay not predicted and <10% protein removed, not reported in other patients, likely pathogenic), consistent with Autosomal Recessive Osteopetrosis (OP-ARO) (All *TNFRSF11A* sequence information is based on GenBank reference sequence NM_003839.3). The pathogenic variants in this case are also in Xue et al focussed on separate subsequent functional work, under the descriptor dysosteosclerosis, on the osteopetrosis spectrum (Xue et al., 2020). A pre-transplant Dual energy X-ray absorptiometry (DXA) scan using Hologic C confirmed markedly elevated Lumbar (L1-L4) Bone Mineral Density (BMD), *Z*-score + 6.3.

Aged 3.1 years, she underwent a haploidentical-maternal HSCT, HLA matching 5/10, bone marrow stem cells (donor had normal bone mineral density). HSCT workup included IgG immunoglobulins 4.99 g/L normal for age. The conditioning regimen comprised rituximab, alemtuzumab, busulfan, fludarabine and cyclophosphamide. The CD34 cell dose administered was 4.29 × 10^6/kg. Hypercalcaemia (adjusted calcium 3.0 mmol/L [2.20–2.70]) occurred on Day 18 post-HSCT, four days ahead of engraftment (Day 22) defined by the first of three consecutive days of neutrophils >0.5 × 10^9/L. Hyperhydration and diuretics for 36 h were ineffective and hypercalcaemia (Fig. 2) worsened to adjusted calcium 4.09 mmol/L(16.4 mg/dL) with hypercalciuria (calcium creatinine ratio 12.30 [N < 0.8]). Denosumab 0.13 mg/kg (1.2 mg; weight 9.2 kg, open orange diamond in Fig. 2) subcutaneous injection was administered on Day 20 post-HSCT. Administration details involved denosumab 60 mg in 1 mL diluted to 10 mL with water-for-injection, of which 0.2 mL (=1.2 mg) was injected. Serum calcium reduced minimally (4.09 to 3.65 mmol/L), raising concern whether the denosumab dose was insufficient or involved incomplete delivery of the extremely small volume. An additional denosumab dose 0.2 mg/kg was administered 4 days later, creating an effective total denosumab dose 0.33 mg/kg which normalised serum calcium (2.51 mmol/L) for 3 weeks. Thereafter symptomatic hypercalcaemia (increased thirst and abdominal pain) continued to recur after several weeks. On some occasions despite weekly to twice weekly biochemical monitoring, symptomatic hypercalcaemia developed extremely rapidly only a few days after a reassuring calcium level. It was therefore challenging to identify the ideal denosumab dosage regimen. Denosumab 0.25 mg/kg (2.4 mg, shaded orange diamonds in Fig. 2) every 4 weeks proved adequate and was transitioned to larger (0.6 mg/kg: solid orange diamonds in Fig. 2) less frequent (every 8 weeks) doses to reduce injection frequency burden to the child. Unfortunately, the larger dose did not increase duration of efficacy and symptomatic severe hypercalcaemia developed rapidly on four occasions, each involving emergency department presentation and inpatient admission (Days 51, 103, 227 and 272 post-HSCT, varying from 6.5 to 7.5 weeks following previous denosumab injection). Denosumab was required and was consistently efficacious (hyperhydration achieved no improvement). From 9 months post-HSCT, dosing frequency was changed to denosumab 0.6 mg/kg (6 mg) every 6 weeks, which proved effective for the following 12 months (Fig. 2). Hypercalcaemia was accompanied by appropriately suppressed PTH 0.6 (normal range 1.6–6.9 pmol/L) and hypercalciuria (urine calcium: creatinine ratio 2.47 and 3.85 [normal range < 0.8]). Bone turnover markers (alkaline phosphatase [ALP], procollagen 1 N-Terminal Propeptide [P1NP] and C-terminal telopeptide of type 1 collagen [CTX]) are shown in Fig. 3. Alkaline phosphatase (ALP), which was low prior to HSCT (indicated by blue arrow; consistent with the intrinsic low turnover rate of osteopetrosis) rose during episodes of hypercalcaemia post-HSCT but overall remained subnormal for 2 years post-HSCT; it has been more consistently in normal range over the last 10 months. Evidence of excess bone breakdown as the cause of the hypercalcaemia was obtained during five instances of hypercalcaemia demonstrated by elevated CTX 0.94, 1.39, 0.99, 1.71 and 1.85 (normal range 0.1–0.5 μg/L) (see lower panel Fig. 3). CTX was assayed immediately prior and 48 h following denosumab falling from 0.99 μg/L (elevated) to 0.37 μg/L (normal), indicating expected response to denosumab (24 months post-HSCT). Tartrate Resistant Acid Phosphatase (TRAP5b) was 11.3 U/L (measured 27 months post-HSCT).

By 18 months post-HSCT, it was expected that the excessive osteoclast activity responsible for hypercalcaemia might have abated allowing denosumab to be withdrawn. We cautiously weaned denosumab, whilst overlapping with introduction of zoledronic acid intravenous infusions to mitigate the potential of the recognised phenomenon of rebound hypercalcaemia on denosumab withdrawal (Boyce, 2017). Despite serial zoledronic acid infusions and frequent monitoring, there was rapid onset of severe (3.81 mmol/L) and symptomatic hypercalcaemia 3 months after discontinuing denosumab (see Fig. 2). This rebound hypercalcaemia from denosumab-washout was treated with both denosumab and zoledronic acid, as was a further occurrence of rebound hypercalcaemia 6 weeks later (adjusted calcium 4.06 mmol/L)

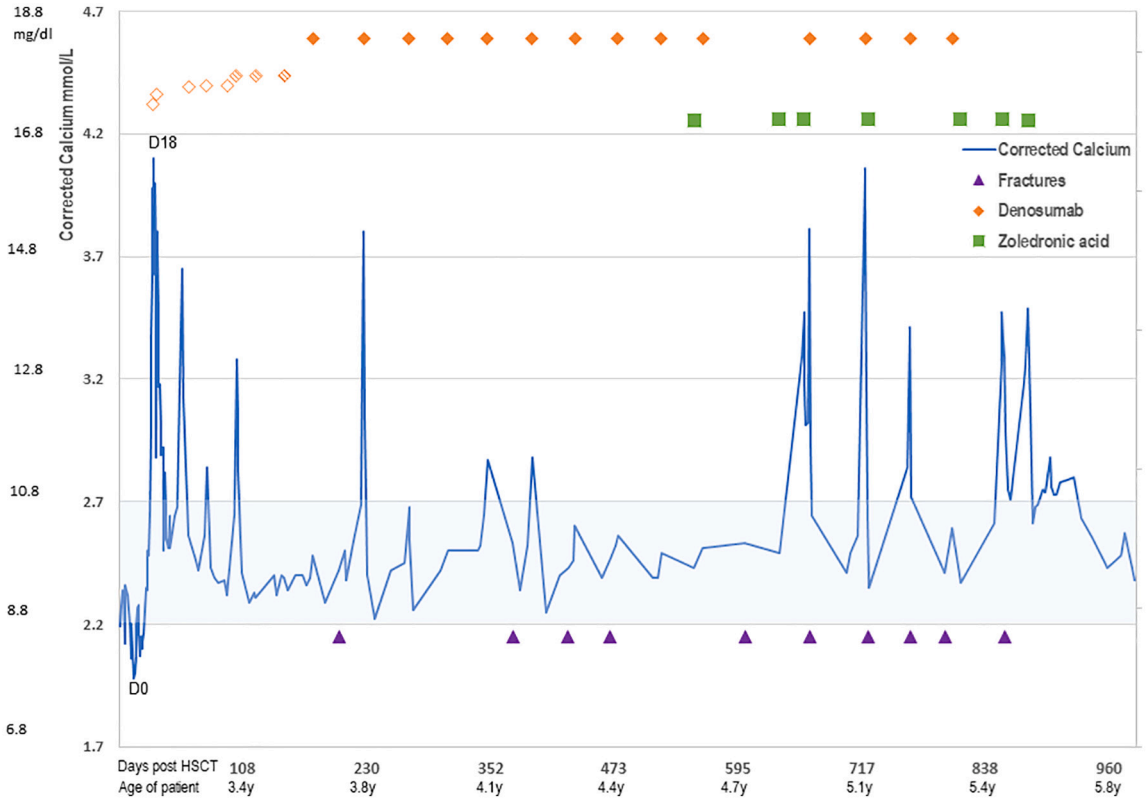

Fig. 2. Episodes of post-HSCT hypercalcaemia, denosumab (orange diamonds ◆) and zoledronic acid (green squares ■) administration and fractures (purple triangles ▲) plotted against time (labelled as both days post-HSCT and age of patient). Serial serum adjusted calcium levels (blue line) plotted against x-axis of Days post-HSCT and age of patient, normocalcaemia (2.2–2.7 mmol/L) indicated by shaded blue range. Calcium data commences 2 week prior to the HSCT, and declines during pre-conditioning phase as expected, falling to mild hypocalcaemia by the time of HSCT (marked as Day 0), then onset of hypercalcaemia with engraftment (D18), with 12 further episodes of hypercalcaemia. Upper section of the figure illustrates denosumab subcutaneous injections (orange diamonds ◆, appearance (open, shaded, solid) and position indicating increased doses) and zoledronic acid infusions (green squares) out to 2.75 years post-HSCT. Lower section of the figure illustrates fracture episodes (purple triangles ▲).

(see Fig. 2); both episodes were associated with hypercalciuria (calcium: creatinine ratio 3.49 and 2.47, at 666 and 722 days (22 and 24 months) post-HSCT respectively). Ultimately, denosumab was administered for 26 months, with zoledronic acid for the latter 8 months thereof. Subsequent to final denosumab injection, two further episodes of significant hypercalcaemia (3.47 and 3.49 mmol/L) required zoledronic acid 0.025 then 0.017 mg/kg infusions respectively. A further episode of mild hypercalcaemia (2.88 mmol/L) was monitored and resolved without intervention. The latest status is normocalcaemia for 3 months (6 months since last denosumab and 4 months since last zoledronic acid).

Nine fragility fractures occurred between 7 and 29 months post-HSCT (nil prior) (Fractures itemised in Table 1 and Radiology shown in Fig. 4). Fractures 1–8 were all low trauma fractures (fell from standing, or for fracture 6: twisted her foot), minimally displaced and managed conservatively. Fracture number 9 differed from previous in mechanism, location, type and intervention required: moderately greater trauma force (fell whilst slowly riding stability tricycle) resulted in an oblique fracture diagonally across an expanded remodelling diaphysis (encompassing diaphyseal new bone growth post-HSCT merging into pre-HSCT osteopetrotic diaphyseal region of femur). This displaced fracture required closed reduction under anaesthetic. All fractures demonstrated normal healing characteristics: clinical resolution within the usual timeframe for normal childhood fractures and with normal callus formation (Fig. 4 panel 2b).

Beyond the above calcium and bone complications, overall progress post-HSCT proceeds well: there has been persistent 100% donor chimerism, normal blood counts, and no other transplant-related complications. Aged 5.9 years, she attends mainstream school with visual impairment educational support. Residual vision has not deteriorated, and hearing remains stable. Linear growth demonstrates normal but not increased growth velocity, i.e. no catch-up growth has occurred: Height SDS -3.7 SDS both just prior to transplant and 2.6 years post-transplant. Appreciable reduction in BMD did not occur in the initial 1.5 years, but is evident 2.5 years post-HSCT (see Table 2). Lateral spine plain radiography 2.4 years post HSCT is unchanged, showing neither progression from mild platyspondyly nor evidence of vertebral fractures. Renal ultrasound was normal pre-transplant, but mild nephrocalcinosis was identified 6 months post-HSCT and remains stable (bilateral grade 1 nephrocalcinosis) on serial monitoring with normal renal function.

3. Discussion

Osteopetrosis is a heterogeneous group of rare skeletal disorders characterised by increased bone density due to defective osteoclast differentiation and function (Wu et al., 2017). Autosomal dominant forms can be relatively mild and usually diagnosed in adulthood, whereas autosomal recessive osteopetrosis (ARO) forms are more severe and typically present in infancy. Our case demonstrates several new learning points relevant to optimal clinical management of the ultrarare subtype of *TNFRSF11A*-related ARO (1–4% of cases of ARO). These include several notable ARO clinical features (failure to thrive, optic atrophy and dental abnormalities), unusual radiographic skeletal changes (specifically loss of corticomedullary differentiation, and prominent medullary lucencies in proximal and distal diaphyses), craniosynostosis and fragility fractures. Three clinical aspects to highlight for further discussion are the initial cranial vault abnormalities, the post-

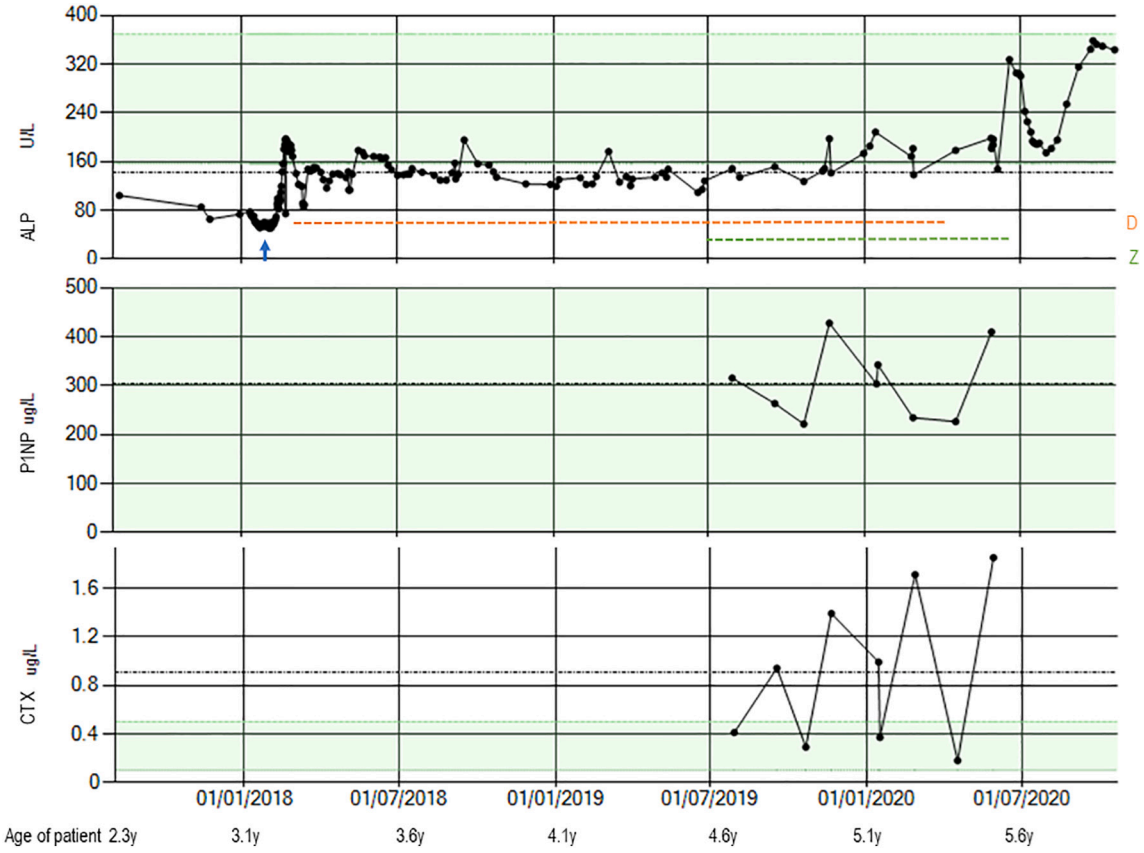

Fig. 3. Bone turnover markers: upper panel shows Alkaline phosphatase (ALP), which was low prior to HSCT (indicated by blue arrow) consistent with the intrinsic low turnover rate of osteopetrosis, then following HSCT rose at episodes of hypercalcaemia but overall remained subnormal for 2 years post-HSCT, then more consistently in normal range over last 10 months. The horizontal dashed orange line indicates the 26 months duration of denosumab and horizontal dashed green line indicates zoledronic acid which overlaps with 8 months of denosumab and indicates total zoledronic acid duration 11 months. Middle panel shows Procollagen N-Terminal Propeptide [P1NP] was normal on all occasions measured providing reassurance against excessive suppression. Lower panel shows C-terminal telopeptide of type 1 collagen [CTX] showed fluctuation with elevated results coinciding with episodes of hypercalcaemia (see text) with normalised levels after denosumab indicating appropriate osteoclast response to denosumab. Normal ranges indicated by green shading in all 3 panels.

Table 1
Nine fragility fractures occurred between 7 and 29 months post-HSCT.

Fracture number	Months post-HSCT	Age (y)	Fractures (nil pre-HSCT)	Fracture details
1	7	3.7	Left Clavicle	Transverse proximal third of diaphysis
2	12	4.1	Left humerus	Transverse proximal third of diaphysis
3	14	4.3	Left fibula	Transverse proximal third of diaphysis
4	16	4.4	Left tibia and fibula	Transverse distal tibial diaphyses and minimal fracture lateral aspect of distal fibular diaphysis
5	20	4.8	Right tibia and fibula	Oblique distal third of tibial diaphysis Transverse distal third of fibula diaphysis
6	24	5.2	Right metatarsals	Transverse distal third of diaphyses of second and third metatarsals
7	25	5.2	Right clavicle	Transverse proximal third of diaphysis
8	27	5.3	Left tibia	Anterior portion of distal tibial metadiaphyseal region
9	29	5.4	Left femur	Oblique diagonal through distal-mid expanded region of diaphysis

HSCT hypercalcaemia and the fragility fractures.

Recognised cranial abnormalities in ARO occur due to increased skull base bone mass causing hydrocephalus, which was not present in our case, and visual impairment from foraminal narrowing (Steward, 2003). Although craniosynostosis is not widely considered as a characteristic component of osteopetrosis, we identified 6 other individual case reports of craniosynostosis in ARO; genetic variants were reported for half the cases: TCIRG1 (n = 2) and OSTEM (n = 1), unreported (n = 3) (Driessen et al., 2003). We propose that craniosynostosis reflects reduced osteoclast activity giving abnormal bone modelling at cranial sutures and is relevant in identifying ARO, since craniosynostosis may present prior to obvious skeletal sclerosis. Our case highlights this diagnostic subtlety, as retrospective review of the initial skull radiographs confirmed no apparent increase density of either skull vault or base in early infancy.

The majority of ARO involve osteoclasts that are present but poorly functioning with compensatory positive feedback loops explaining the 'osteoclast-rich' appearances on bone biopsy; genes involved are *CA2, TCIRG1, CLCN7, OSTM1, PLEKHM1, SNX10* (Penna et al., *2019*). In the rarer subgroup of OP-ARO, loss-of-function mutations prevent osteoclast formation, for which two causative genes have been identified: *TNFSF11* and *TNFRSF11A*. The cause of absent osteoclasts in *TNFSF11*-related ARO is the lack of RANKL to induce pre-osteoclast differentiation. By contrast, *TNFRSF11A* encodes the membrane-anchored RANK protein in the pre-osteoclast itself, without which pre-osteoclasts are intrinsically abnormal and unable to differentiate. This specific feature underpins the uniqueness of the *TNFRSF11A*-related OP-ARO as the type most likely to

Fig. 4. Fragility fractures post-HSCT. Plain radiographs numbering corresponds with fracture episode chronology listed in Table 1. Arrows mark the fracture sites, in addition, all images show evidence of the underlying osteopetrotic changes of intra-medullary lucencies and diffuse sclerotic appearance similar to pre-HSCT evident in Fig. 1 images. 1: Left clavicle: transverse minimally displaced fracture through the medial third of the left clavicle diaphysis. 2a: Left humerus: transverse lucency across proximal third of humeral diaphysis. 2b is 7 weeks after image 2 and demonstrates proximal left humeral fracture with cortical remodelling, alignment preserved, sclerosed fracture plane and callus formation, pronounced on medial aspect. 3: left tibia and fibula: transverse fracture at proximal third of fibular diaphysis linear. 4: left tibia and fibula: upper arrow against proximal third of fibular diaphysis shows healing fracture from panel 3 and lower two arrows show new minimally displaced fractures through distal tibial and fibular diaphyses. 5: Right tibia and fibula: minimally-displaced oblique fracture of distal tibial diaphysis and an undisplaced transverse fracture of distal fibular diaphysis. 6: Right foot: non-displaced fracture through 2nd & 3rd metatarsals. 7 Right clavicle: Transverse fracture across proximal third. 8a Left tibia: fracture not evident on this AP image (so no arrow) whereas 8b (lateral image) shows non-displaced linear lucency evident through anterior distal tibia. 9 Left Femur: two arrows show upper and lower margins of oblique displaced fracture through expanded distal femoral diaphysis. This images 2.5 years post-HSCT also demonstrates improvement of metaphyseal contour and quality in comparison to pre-HSCT image to its right, with lessening of the medullary lucencies and loss of Erlenmeyer flask type deformity. 10: (lower right) does not contain a fracture but shown here in addition to Fig. 1 (panel 1) to facilitate comparison of left femur diaphysis pre-HSCT against progressively changed in bone appearance post-transplant.

Table 2
Serial bone mineral density DXA scans, performed using Hologic C.

Age (years)	Years post-HSCT	Whole body less head bone mineral density (g/cm^2)	Lumbar spine (L1–4) bone mineral density (g/cm^2)	Lumbar spine Z score
2.8		Unavailable	0.934	+6.3
4	0.9	Unavailable	1.052	+6.1
4.6	1.5	0.689	1.133	+6.1
5.6	2.5	0.625	1.055	+5.2

involve severe hypercalcaemia following HSCT, as the transition from completely non-functional pre-osteoclasts to the engraftment of normal well-functioning RANK-secreting pre-osteoclasts permits a sudden increase in osteoclast activity. Osteoclasts break down pre-existing excess bone, releasing significant circulating excess calcium.

Life-threatening hypercalcaemia post-HSCT for OP-ARO is a known complication. Reported overall prevalence ranges from 16 to 40%, with higher risk 60% in patients older than 2 years of age attributed to their higher bone mass (Martinez et al., 2010; Shroff et al., 2012; Pangrazio et al., 2012; Driessen et al., 2003). In the OP-ARO subset (due to *TNFRSF11A* mutations), hypercalcaemia post-HSCT seems to have an even higher prevalence, earlier onset, and be both recurrent and more severe (Martinez et al., 2010; Penna et al., 2019). This presents clinicians with significant challenges regarding effective treatment options which until recently were limited to hyperhydration, furosemide, calcitonin, glucocorticoids, bisphosphonates and haemofiltration (Basok et al., 2018).

The emergence of denosumab, first approved for use in adults in 2010, as a potent anti-resorptive agent has provided an exciting new therapeutic option which more directly targets the pathophysiology of the hypercalcaemia. This human monoclonal antibody binds the RANK receptor with high affinity and specificity. It blocks RANKL binding, preventing osteoclast differentiation and hence reducing bone resorption. Denosumab is licensed for use in adults for post-menopausal osteoporosis, giant cell tumours, and hypercalcemia due to malignancy and bone metastases (Boyce, 2017; Polyzos et al., 2019). There is emerging but cautious use of denosumab in paediatrics: clinical research trials in osteogenesis imperfecta (OI) and limited off-license use (Boyce, 2017; Polyzos et al., 2019). Paediatric doses have differed widely: most commonly 1 mg/kg every 6 months, shorter intervals of 10 weeks in Type VI OI to manage breakthrough hypercalcaemia (Trejo et al., 2018)

and a range of doses in different bone conditions; along with this relatively frequent administration of 0.6 mg/kg every 6 weeks in post-HSCT hypercalcaemia in our case.

Shroff et al first described denosumab to treat post-HSCT hypercalcaemia in two paediatric patients with OP-ARO due to *TNFRSF11A* mutations (Shroff et al., 2012). These patients were treated with denosumab 0.13–0.27 mg/kg, appreciably lower doses than the 1 mg/kg regimen used in paediatric OI studies. In our small (<10 kg) patient, we elected to treat cautiously initially, using the lower dose 0.13 mg/kg (1.2 mg) subcutaneously. However, effective control of ongoing hypercalcaemia was not achieved until titration through several dosages to 0.6 mg/kg once every 6 weeks for 18–24 months. This clinical efficacy duration of 6 weeks fits with evidence that bone turnover markers return to pre-treatment levels 6–8 weeks post denosumab (Boyce, 2017). The degree of rebound hypercalcaemia appeared uninfluenced by denosumab dosage; the challenge was to reach duration of control that avoided overly frequent painful injections for this child. We propose use of denosumab 0.6 mg/kg at 6 week intervals, higher than previously reported, in severe cases in the unique cohort of OP-ARO post-HSCT for medium-term control of hypercalcaemia.

Commencing denosumab for RANK-related *TNFRSF11A* OP-ARO post-HSCT hypercalcaemia is an intuitive choice and is effective precisely because it directly targets the RANK signalling pathway now restored by HSCT. The temporary-reversible nature of denosumab was preferred over the potentially toxic bisphosphonate effect on engrafting stem cells. But this initial solution can be followed by the dilemma of how to safely discontinue. Upon ceasing denosumab, the monoclonal antibody no longer blocks the RANK pathway, unleashing a potentially amassed pool of pre-osteoclasts. Rebound hypercalcaemia is a recognised complication following denosumab discontinuation in adults and children, particularly in high bone turnover conditions, e.g. giant cell tumours, Paget's disease and fibrous dysplasia (Boyce, 2017). This rebound hypercalcaemia of denosumab washout was probably amplified by the underlying OP-ARO high bone mass, and hypothetically compensatory over-expression of RANKL proposed in RANK-related ARO (Sobacchi et al., 2013). These may all have contributed to severe hypercalcemia recurring whilst withdrawing denosumab, requiring 8 months concurrent zoledronic acid to control. Elevated bone turnover marker CTX indicates bone breakdown, inferring osteoclast activity, common to all mechanisms. The serum tartrate resistant acid phosphatase (TRAP5b) 11.3 U/L may indicate reasonable osteoclast numbers at 2.3 years post-HSCT; although there are neither reference ranges young children or young children with ARO post-HSCT, 11.3 is reassuringly close to 13–23 U/L (normal range 7.5-10 years (Whyte et al., 2010)). We hypothesise that longterm denosumab may have suppressed remodelling (ALP normalisation took 2 years post-HSCT). However, the medical reality was dramatic hypercalcaemia causing systemic symptoms, where prompt control was essential to reduce risk of nephrocalcinosis progressing to renal impairment. Lower doses may have minimised suppression, but they resulted in extremely frequent injections that were not tolerable for the child. Our case does raise the possibility that whilst denosumab is a rational solution for initial management it may perpetuate hypercalcaemia. So potentially addition of zoledronic acid earlier, e.g. after 8–12 months rather than 18 months, may be advisable. Overall, we attribute the extent of hypercalcaemia predominantly to the excessiveness of bone mass accumulated by the older age of transplant, a concept supported by the literature (Orchard et al., 2015).

Restoration of osteoclast activity is an important outcome of HSCT for osteopetrosis. Skeletal remodelling in our case is indicated by hypercalcaemia and bone turnover markers. Progressive reduction of elevated bone mass is expected, although no other reports used DXA to quantify bone density. Our case highlights that reduction in DXA bone density may take a longer time frame to emerge - evident by 2.5 years, but not at 1.5 years post-HSCT (Table 2). Long duration of skeletal remodelling offloading excessive calcium can be attributed to the extent of excessive bone mass accumulated by older age at transplant (Orchard et al., 2015). We had considered whether transplantation from a haploidentical donor rather than a homozygous normal donor did not achieve full bone correction. We discounted this hypothesis as HSCT is often done without apparent issue from parental or sibling carriers in other forms of osteopetrosis and secondly our maternal donor's normal bone mineral density provides reassurance. Functional studies on this child's pathogenic variants have very recently been published (Xue et al., 2020), giving some insight into osteoclast dysfunction mechanisms and highlighting that osteopetrosis and dysosteosclerosis comprise a spectrum. Subsequent studies could further elucidate our unique case in due course.

Our patient experienced 9 fragility fractures 7–29 months post-HSCT but none prior to transplant. This contrast pre and post HSCT may be coincidental, since fractures are a recognised feature of the natural history of osteopetrosis without stem cell transplant, due to the inherently brittle marble-like bone (Sobacchi et al., 2013). Comparative post-HSCT fracture data is an acknowledged gap in follow-up studies (Orchard et al., 2015). It is plausible that the post-HSCT fractures are a consequence of bone turnover with normalised osteoclast function and bone physiology. It is notable that the long bone fractures in our case occurred at the junction of new diaphyseal bone growth post-HSCT with pre-existing 'marble-like' diffuse sclerotic bone (Figs. 1 and 4), potentially where now restored osteoclast aims to remodel that abnormal bone. This junctional location is similar to 'stress-riser' fractures with bisphosphonate treated bone and medication-naïve bone. There is no evidence to indicate whether denosumab osteoclast inhibition increases or attenuates fracture risk in OP-ARO. Nevertheless, the impact of recurring fragility fractures was significant for this young child and influenced our pragmatic clinical decision to attempt to wean denosumab and then zoledronic acid therapies to avoid ongoing bone suppression and inhibition of bone remodelling. Since discontinuing both therapies, one episode of mild self-resolving hypercalcaemia suggests bone remodelling off-loading calcium. Ongoing surveillance will monitor bone quality improvement over the coming years.

4. Conclusion

Post-HSCT for OP-ARO, intrinsic osteoclast drive breaks down calcium laden osteopetrotic bone, as remodelling strives to progressively normalise the skeleton. Our case demonstrates the challenge in achieving optimal treatment to permit sufficient bone turnover for skeletal remodelling, whilst sufficiently suppressing bone turnover to avoid life-threatening hypercalcaemia. Denosumab is effective for medium term use in OP-ARO post-HSCT to combat recurrent hypercalcaemia. Thereafter, withdrawal is relevant to permit engrafted osteoclasts to facilitate skeletal remodelling. Judicious withdrawal entails more than the single bisphosphonate administration to 'seal in calcium' effective in low bone mass conditions, e.g. OI, and involves prolonged concurrent zoledronic acid (8 months), during which vigilance for rapid onset severe hypercalcaemia must be maintained.

Funding

This research did not receive any specific grant from funding agencies in the public, commercial, or not-for-profit sectors.

Ethics statement

Our research complies with all relevant national regulations and institutional policies. Informed consent was obtained from the parents of the child for inclusion in this research.

CRediT authorship contribution statement

TTM: Writing - original draft, review & editing, PS: Resources, SFS: Resources, Writing - review & editing, CS: Resources, Writing - review &

editing, CPB: Conceptualization, Resources, Supervision, Writing - review & editing, revisions, Visualization. All authors have approved the final version of the manuscript.

Declaration of competing interest

None.

References

Basok, A.B., Rogachev, B., Haviv, Y.S., Vorobiov, M., Jun. 2018. Treatment of extreme hypercalcaemia: the role of haemodialysis. BMJ case reports 2018. https://doi.org/10.1136/bcr-2017-223772.

Boyce, A.M., Aug. 2017. Denosumab: an emerging therapy in pediatric bone disorders. Current Osteoporosis Reports 15 (4), 283–292. https://doi.org/10.1007/s11914-017-0380-1.

Driessen, G.J.A., et al., Oct. 2003. Long-term outcome of haematopoietic stem cell transplantation in autosomal recessive osteopetrosis: an EBMT report. Bone Marrow Transplant. 32 (7), 657–663. https://doi.org/10.1038/sj.bmt.1704194.

Martinez, C., et al., May 2010. Characterization and management of hypercalcemia following transplantation for osteopetrosis. Bone Marrow Transplant. 45 (5), 939–944. https://doi.org/10.1038/bmt.2009.277.

Orchard, P.J., et al., Jul. 2015. Hematopoietic stem cell transplantation for infantile osteopetrosis. Blood 126 (2), 270–276. https://doi.org/10.1182/blood-2015-01-625541.

Pangrazio, A., et al., 2012. RANK-dependent autosomal recessive osteopetrosis: characterization of five new cases with novel mutations. Journal of Bone and Mineral Research. https://doi.org/10.1002/jbmr.559.

P. G. Paul, F. N.A, S. Korula, S. Mathai, B. George, and A. Simon, "Hypercalcemia as a post stem cell transplantation complication in children with osteopetrosis - a single centre experience," *Hormone Research in Paediatrics*, vol. 91, no. Supplement 1, pp. 211–211, Aug. 2019, Accessed February 26, 2020. [Online]. Available: http://abstracts.eurospe.org/hrp/0092/hrp0092P1-169.

Penna, S., Capo, V., Palagano, E., Sobacchi, C., Villa, A., Feb. 2019. One disease, many genes: implications for the treatment of osteopetroses. Front. Endocrinol. 10, 85. https://doi.org/10.3389/fendo.2019.00085.

Polyzos, S.A., Makras, P., Tournis, S., Anastasilakis, A.D., Dec. 2019. Off-label uses of denosumab in metabolic bone diseases. Bone 129, 115048 [Online]. Available: https://linkinghub.elsevier.com/retrieve/pii/S8756328219303382.

Richards, S., et al., May 2015. Standards and guidelines for the interpretation of sequence variants: a joint consensus recommendation of the American College of Medical Genetics and Genomics and the Association for Molecular Pathology. Genetics in Medicine 17 (5), 405–423. https://doi.org/10.1038/gim.2015.30.

Shroff, R., Beringer, O., Rao, K., Hofbauer, L.C., Schulz, A., 2012. Denosumab for post-transplantation hypercalcemia in osteopetrosis. New Engl J Med 367, 1766–1767. https://doi.org/10.1056/NEJMc1210783.

Sobacchi, C., Schulz, A., Coxon, F.P., Villa, A., Helfrich, M.H., 2013. Osteopetrosis: genetics, treatment and new insights into osteoclast function. Nature Reviews Endocrinology. https://doi.org/10.1038/nrendo.2013.137.

Steward, C.G., 2003. Neurological aspects of osteopetrosis. Neuropathol. Appl. Neurobiol. 29, 87–97. https://doi.org/10.1046/j.0305-1846.2003.00474.x.

Trejo, P., Rauch, F., Ward, L., 2018. Hypercalcemia and hypercalciuria during denosumab treatment in children with osteogenesis imperfecta type VI [Online]. Available: http://www.ismni.org.

Whyte, M.P., Kempa, L.G., McAlister, W.H., Zhang, F., Mumm, S., Wenkert, D., Nov. 2010. Elevated serum lactate dehydrogenase isoenzymes and aspartate transaminase distinguish Albers-Schönberg disease (Chloride Channel 7 deficiency Osteopetrosis) among the sclerosing bone disorders. J. Bone Miner. Res. 25 (11), 2515–2526. https://doi.org/10.1002/jbmr.130.

Wu, C.C., et al., Sep. 01, 2017. Diagnosis and management of osteopetrosis: consensus guidelines from the osteopetrosis working group. Journal of Clinical Endocrinology and Metabolism 102 (9), 3111–3123. https://doi.org/10.1210/jc.2017-01127. Oxford University Press.

Xue, J.Y., et al., Oct. 2020. The third case of TNFRSF11A-associated dysosteosclerosis with a mutation producing elongating proteins. J. Hum. Genet. 1–7. https://doi.org/10.1038/s10038-020-00831-8.